Morphology and Texture Development of Uniaxially Stretched Poly(ethylene naphthalene-2,6-dicarboxylate)

A. Douillard,[1] C. Hakme,[1] L. David,[1] I. Stevenson,[1] G. Boiteux,[1] G. Seytre,[1] T. Kazmierczak,[2] A. Galeski[2]

[1]*Laboratoire des Matériaux Polymères et des Biomatériaux, UMR CNRS 5627, Université Claude Bernard–Lyon 1, Bat. ISTIL, 43, Bd du 11 novembre 1918, 69622 Villeurbanne cedex, France*
[2]*Centrum Badan Molekularnych I Makromolekularnych, 90-363 Lodz, ul.Sienkiewicza 112 Poland*

Received 22 February 2006; accepted 14 April 2006
DOI 10.1002/app.24758
Published online in Wiley InterScience (www.interscience.wiley.com).

ABSTRACT: The texture development of PEN films with different semicrystalline morphologies have been studied by X-ray diffraction. These different structures have been obtained by uniaxially stretching PEN amorphous films at 100 and 160°C (below and above T_g) at different drawing ratios. Samples have also been characterized by DSC to determine the crystallinity ratios, the crystallization, and melting temperatures. To define the orientation of crystallites in the oriented samples, pole figures have been constructed, as a function of temperature and drawing ratio (DR) in the range 1.5–4. In the range from DR = 2 to 4 the orientation is clearly uniplanar-axial. At $T_{draw} = 100$°C the crystallinity shown by DSC analysis is higher than the sample stretched at 160°C. The orientation is also higher when samples are stretched at 100°C. The naphthalene rings mainly stay in the plane of the film with a lower fraction perpendicular to the plane of the film. © 2006 Wiley Periodicals, Inc. J Appl Polym Sci 103: 395–401, 2007

Key words: morphology; X-rays; pole figure; texture; orientation; poly(ethylene naphthalene-2,6-dicarboxylate) (PEN); differential scanning calorimetry (DSC)

INTRODUCTION

As poly(ethylene naphthalene-2,6-dicarboxylate) (PEN) is largely used in the form of thin films which can be obtained by uniaxial or biaxial stretching, the understanding of the evolution of its morphology and orientation with temperature and stretching conditions is essential to adjust its properties for a given application.[1–4] The complex orientation of industrially stretched PEN during a two step biaxial process was studied by the building of pole figures in a previous paper.[5] The establishment of relationships between microstructure and properties (dielectric or mechanical) is not straightforward, due to the complexity of the morphology. Moreover, the morphology itself is difficult to interpret as a function of processing parameters. The aim of this work is to study the effect of a homemade uniaxial stretching on PEN films. This can be viewed as a thermomechanical treatment yielding a more simple morphology, but also the first step of a more complicated biaxial stretching.

During the last decade, several papers have been devoted in literature to the microstructure of uniaxially drawn PEN. Murakami et al.[4] have studied orientation and structural change of amorphous PEN during uniaxial drawing and/or heating. Stretching at temperature lower than T_g (120°C) produces oriented structure with neck formation. On the other hand, drawing at 150°C ($> T_g$) gives directly a crystalline fibrous structure with uniaxial planar orientation in which the naphthalene ring is parallel to the film plane.

EXPERIMENTAL

PEN samples were obtained from Du Pont de Nemours (Luxembourg) as amorphous films with a thickness of 300 μm. These films were stretched uniaxially at an initial speed of 0.02 s^{-1} (50 mm/min with a distance between clamps of $l_o = 40$ mm) using a tensile test machine (MTS 2/M) equipped with a thermoregulated chamber at two different drawing temperatures, below and above T_g, respectively, at 100 and 160°C. Four macroscopic drawing ratio (DR = l/l_o) were applied: 1.5, 2, 3, and 4. The DR of the different samples was evaluated at a more local scale by means of the deformation of a fine grid stamped on the films.[6] The correspondence between macroscopic and experimentally measured drawing ratios is reported in Table I.

The WAXS system used to obtain pole figures has been described elsewhere,[5] including the POD software. The slit opening allowing to collect scattered beam was within ±0.155° around the fixed 2θ angle. As in Ref. 5, DSC measurements were carried out using a 2920 TA Instruments (range from 50 to 300°C with a heating rate of 10 K/min, with samples of about 5 mg).

Correspondence to: I. Stevenson (isabelle.stevenson@univ-lyon1.fr).
Contract grant sponsor: MIRA.

TABLE I
Correspondence Between Macroscopic and Real Drawing Ratio of the Samples Used in This Study

Macroscopic DR	Sample	Real DR 100°C	Sample	Real DR 160°C
1.5	1001	1.6	1601	1.7
2	1002	3.2	1602	3.5
3	1003	4.3	1603	4.8
4	1004	4.8	1604	5.3

CRYSTALLOGRAPHIC DATA OF PEN

The crystallographic data[7] for the triclinic P-1 unit cell of the α phase are given by the unit cell parameters with $a = 6.51$ Å, $b = 5.75$ Å, $c = 13.2$ Å, $\alpha = 81°20'$, $\beta = 144°$, $\gamma = 100°$ (Fig. 1), the unit cell volume is $V = 285.6$ Å^3, the calculated density of the crystalline phase is 1.407 g/cm^3. Crystalline and amorphous linear absorption coefficient at the Cu Kα wavelength are: $\mu_C = 9.09$ cm^{-1} and $\mu_A = 8.3433$ cm^{-1}, respectively. The previously calculated coordinates of the vectors normal to the (h k l) planes[5] in the α phase in the orthonormal reference, using Mencik's[7] results, are reported in Table II.

The (1 0 0), (0 1 0), and (−1 1 0) reticular planes of the α phase having the highest diffracted intensities were studied. The planes corresponding to the set, (2 1 −1), (−2 2 5), (−1 1 5), (−3 0 6), (−2 0 6) and located at $2\theta = (43.5 \pm 0.155)°$ were also studied.* Table II also presents interreticular distances, diffraction angles of several reticular planes occurring in the pole figures, and the coordinates of the normal $\vec{n}_{h\ k\ l}$ and the normal vector perpendicular to the naphthalene planes. Figure 2 displays the unit cell vectors in the reference coordinate axis, together with the reciprocal unit vectors. Figure 3 schematically shows the location of poles on the projection sphere. The machine direction (MD) is the drawing direction and the transverse direction (TD) is in the film plane and perpendicular to MD. The normal direction ND is perpendicular to the plane of the film. For this particular representation, it is assumed, as found later, that the $\vec{c}$ axis is mainly in the MD direction and the naphthalene chain plane is perpendicular to the (MD)/(TD) plane, i.e., in the MD direction.

Some interferences can occur in the pole figures, namely (−1 −1 1) with (1 0 0) and (−1 0 1) with (0 1 0). The (−1 −1 1) pole is not visible on the (1 0 0) pole figures, due to a quite different interreticular distance. As regards the interference between (−1 0 1) and (0 1 0), the low value of the structure factor of (−1 0 1) introduces a minor influence although the pole should appear on (0 1 0) pole figures.

The respective dihedral angles between the reticular planes used or between the normal (modulo 180°) have been calculated and are reported in Table III. Thus, the intersection of (1 0 0), (0 1 0) reticular planes redefines the $\vec{c}$ axis direction. The angle between the normal to the chain plain and the normal to (−1 1 0) is 7.11° (see Fig. 1), and then the (−1 1 0) plane has the highest electronic density, i.e., structure factor F (cf Ref. 7).

The morphology and texture of uniaxially stretched PEN films can then be analyzed to relate their oriented structure to their thermomechanical history. First of all, pole figures give the orientations of the unit cells. To compare oriented samples with different drawing ratios and drawing temperatures, the mean square cosine of the angle between the normal $\vec{n}_{h\ k\ l}$ and the ND direction, $\langle\cos^2(\varphi_{h\ k\ l,\mathrm{MD}})\rangle$, and relative orientation functions are determined for a suited set of reticular planes, to characterize the orientation of fiber axis c and the naphthalene planes.

Corrections of intensities were made, i.e., the background scattering and the sample absorption were calculated. In these conditions, comparison of the mean square cosine should allow a classification of the orientations of samples versus DR and temperature.

According to Alexander,[8] the axes of the orthonormal reference attached to the unit cell are Oz (parallel to $\vec{c}$ and chain axis), Ox and Oy, and these axes are chosen so that $\vec{a}$ is in the (Ox,Oz) plane. For a given family of planes, the parameters are then the cosines angles between the reference direction OZ and the Ox, Oy, and Oz directions, namely $\langle\cos^2(\varphi_{Ox,OZ})\rangle$, $\langle\cos^2(\varphi_{Oy,OZ})\rangle$, and $\langle\cos^2(\varphi_{c,OZ})\rangle$. For a given ($h$ k l) plane the orientation $\vec{n}_{h\ k\ l}$ is given by:

$$\langle\cos^2(\varphi_{h\ k\ l,OZ})\rangle = \langle u\ \cos(\varphi_{Ox,OZ}) + v\ \cos(\varphi_{Oy,OZ}) + w\ \cos(\varphi_{c,OZ})\rangle^2, \quad (1)$$

where u, v, w being the coordinates of the normal to the (h k l) plane $\vec{n}_{h\ k\ l}$ in the [O x,y,z] reference. These

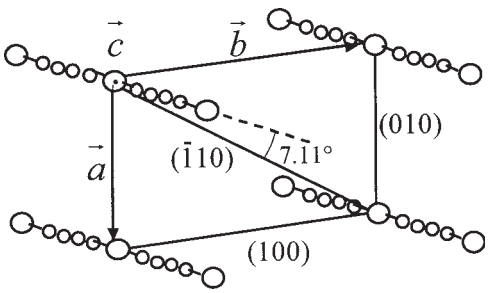

Figure 1 End view of the unit cell of the α crystal with c axis perpendicular to the figure plane.

*In a previous paper,[5] the reticular planes of the α phase having the highest diffracted intensities were studied: (1 0 0), (0 1 0), (−1 1 0) and also the plane assumed to be the (−2 1 0). It was finally not taken in account for complete disagreement. This was due to a misunderstanding in transmission of results and the measurement was made at $2\theta = (43.5 \pm 0.155)°$ instead of $2\theta = 49.2°$ as assumed. As said before, the reticular planes corresponding to this scattering angle were the set (2 1 −1), (−2 2 5), (−1 1 5), (−3 0 6), and (−2 0 6). It is worth noting that results concerning this ''(−2 1 0) pole'' in Ref. 5 are in complete agreement with the finally selected poles.

TABLE II
Crystallographic and Diffraction Data for α Crystals PEN Including the Coordinates of the Normal to the Naphthalene Ring Plane

($h\ k\ l$)	2θ (°)[a]	$d_{h\ k\ l}$ (Å)	F_{calc}[b]	$u = n_x$	$v = n_y$	$w = n_z$
(1 0 0)	23.339	3.8113	62	0.9960277	0.008904348	0
(1 −1 1)	23.761	3.7446	21	−0.5881436	−0.7573721	0.2836803
(0 1 0)	15.651	5.6618	46	0	1	0
(−1 0 1)	15.618	5.6736	8	−0.891248	−0.145442	0.429818
(−1 1 0)	27.012	3.3008	84	−0.8626074	0.505874	0
(2 1 −1)	43.564	2.0775	20	−0.8692136	−0.4687196	0.15733834
(−2 0 6)	42.481	2.1279	18	0.2190755	−0.1284332	0.9672181
(−1 1 5)	43.516	2.0796	31	0.5407395	0.2950978	0.7877297
(−2 2 5)	43.455	2.0824	34	$-2.74155 \cdot 10^{-3}$	0.6146498	0.7887954
(−3 0 6)	44.251	2.0468	33	−0.324171	−0.171356	0.9303495
Naphthalene plane	–	–	–	−0.9185828	0.3952248	0

[a] For the CuKα wavelength.
[b] From Ref. 4.

cosines values are related by the orthogonality relationship:

$$\langle \cos^2(\varphi_{Ox,OZ})\rangle + \langle \cos^2(\varphi_{Oy,OZ})\rangle + \langle \cos^2(\varphi_{c,OZ})\rangle = 1 \quad (2)$$

In general, the measurements of $\langle \cos^2(\varphi_{h\ k\ l,OZ})\rangle$ for five reticular planes are necessary to deduce the values of $\langle \cos^2(\varphi_{Ox,OZ})\rangle$, $\langle \cos^2(\varphi_{Oy,OZ})\rangle$, and $\langle \cos^2(\varphi_{c,OZ})\rangle$ for the further evaluation of the orientation of any ($h\ k\ l$) plane through the value of $\langle \cos^2(\varphi_{h\ k\ l,OZ})\rangle$, since u, v, and w can be calculated from the knowledge of the crystal structure. These measurements are reduced to three for a ($h\ k\ 0$) set. Accordingly, the (1 0 0), (0 1 0), and (−1 1 0) set yields the relevant mean square cosines from the scalar product $\vec{n}_{h\ k\ l}\overrightarrow{OZ}$, i.e., the development of eq. (1):

$$\begin{cases} \langle \cos^2(\varphi_{100,OZ})\rangle = 0.9921\langle \cos^2(\varphi_{Ox,OZ})\rangle + 0,0079\langle \cos^2(\varphi_{Oy,OZ})\rangle + 0,1774\langle \cos(\varphi_{Ox,OZ})\cos(\varphi_{Oy,OZ})\rangle \\ \langle \cos^2(\varphi_{010,OZ})\rangle = \langle \cos^2(\varphi_{Oy,OZ})\rangle \\ \langle \cos^2(\varphi_{-110,OZ})\rangle = 0,7441\langle \cos^2(\varphi_{Ox,OZ})\rangle + 0,2559\langle \cos^2(\varphi_{Oy,OZ})\rangle - 0,8727(\varphi_{Ox,OZ})\cos(\varphi_{Oy,OZ})\rangle \end{cases} \quad (3)$$

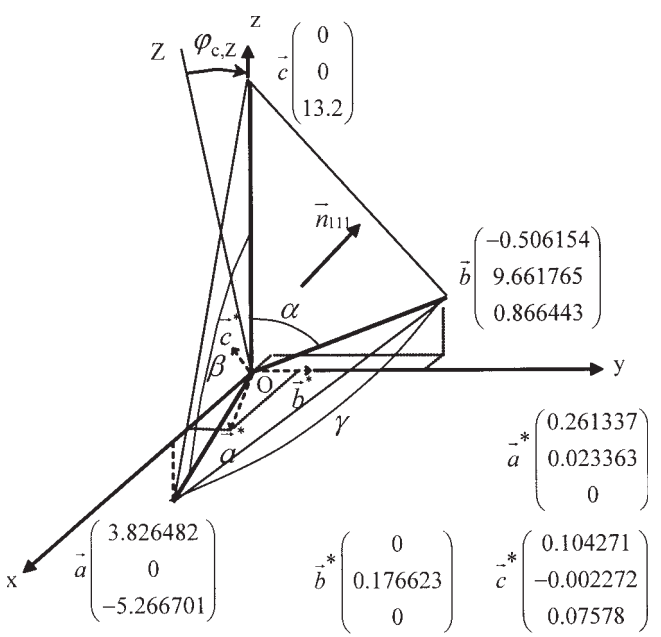

Figure 2 Reference axes attached to the unit cell (*Ox*, *Oy*, *Oz*), and reference axis (*OZ*) for orientation determination, together with the coordinates of unit cell vectors and corresponding reciprocal vectors.

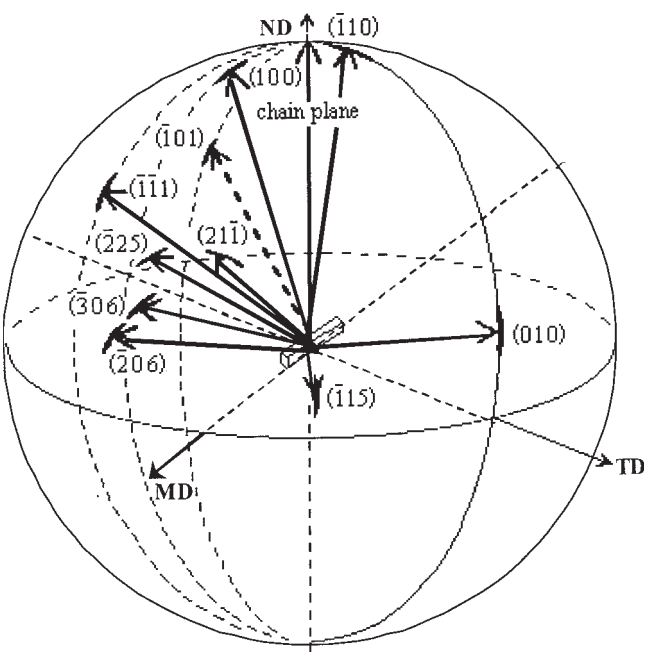

Figure 3 Schematic representation of poles on the stereographic sphere, corresponding to the most probable orientation in PEN after stretching.

TABLE III
Dihedral Angles Between Reticular Planes in the α Form

(*h k l*)	(1 0 0)	(1 −1 1)	(0 1 0)	(−1 0 1)	(−1 1 0)	(2 1 −1)	(−2 0 6)	(−1 1 5)	(−2 2 5)	(−3 0 6)
(1 0 0)										
(1 −1 1)	49.21									
(0 1 0)	84.89	40.77								
(−1 0 1)	25.77	40.87	81.64							
(−1 1 0)	35.50	81.87	59.61	45.96						
(2 1 −1)	24.84	24.84	62.85	24.44	59.16					
(−2 0 6)	78.07	75.95	82.62	76.16	75.29	88.74				
(−1 1 5)	55.61	71.45	72.84	79.87	71.51	61.03	32.60			
(−2 2 5)	87.01	76.11	52.01	75.40	71.74	80.70	46.89	36.74		
(−3 0 6)	70.24	54.24	80.14	44.47	78.88	59.44	31.70	59.54	50.99	
Naphthalene plane	28.39	76.06	66.72	40.44	7.11	52.18	104.60	112.34	75.79	76.70

In turn, the mean square cosines $\langle\cos^2(\varphi_{100,OZ})\rangle$, $\langle\cos^2(\varphi_{010,OZ})\rangle$, and $\langle\cos^2(\varphi_{-110,OZ})\rangle$ of the chain axis can be calculated from:

$$I(\varphi) = \int_0^{2\pi} I(\varphi, \psi, \theta_{h\,k\,l}) d\psi$$

and

$$\left\langle \cos^2(\varphi_{h\,k\,l,OZ}) \right\rangle = \frac{\int_0^{\pi/2} I(\varphi) \sin\varphi \cos^2\varphi \cdot d\varphi}{\int_0^{\pi/2} I(\varphi) \sin\varphi \cdot d\varphi} \quad (4)$$

where *OZ* is the reference direction (e.g., MD, TD, or ND directions), φ is the meridian coordinate (φ = ±90 at the poles, where *OZ* is the pole axis), and ψ is the latitude coordinate in the polar representation, which are in correspondence with the orientation angles of the film, respectively, to the incident beam and diffraction plane.[8]

Practically, the integrals above correspond to the summations:

$$I(\varphi) = \sum_{\psi=0}^{180} I(\varphi, \psi) \Delta\psi$$

and

$$\left\langle \cos^2(\varphi_{hkl,OZ}) \right\rangle = \frac{\sum_0^{90} I(\varphi) \sin(\varphi) \cos^2(\varphi) \Delta\varphi}{\sum_0^{90} I(\varphi) \sin(\varphi) \Delta\varphi} \quad (5)$$

TABLE IV
DSC Characterization Results for Amorphous and Stretched PEN

Sample	T_c (°C)	T_m (°C)	ΔH_{crys} (J/g)	ΔH_{melt} (J/g)	X_c (%)
Amorphous	181	268	120	120	0
100 1	174	267	122	125	2.6
100 2	142	267	34	90	29.9
100 2	–	267	–	96	30.0
100 3	–	267	–	93	30.1
160 1	177	268	126	130	2.3
160 2	169	267	–	96	12.0
160 3	–	267	–	101	18.9
160 4	–	267	–	108	22.7

RESULTS AND DISCUSSION

The DSC crystallinity results for the samples studied are given in Table IV. Figure 4 shows a selection of thermograms obtained for different DR values at 1 0 0 and 160°C. It is clear that low stretched samples are not completely crystallized but samples stretched at a DR above 3 at 160 or 100°C appear well crystallized as there is no DSC crystallization peak.[6]

The general schematic view of (1 0 0), (0 1 0), and (−1 1 0) reticular plane pole figures (respectively, Figs. 5–7) for sample 1604 shows that the orientation of crystals is uniaxial in the film plane, the $\vec{c}$ axis of the crystals being oriented close to the MD. The multiple pole figure for (2 1 −1), (−3 0 6), (−1 1 5), (−2 2 5), and also (−2 0 6) (Fig. 8) can be fully indexed in agreement with Figure 3. Nevertheless, PEN films show large variation of texture according to the temperature and the drawing ratio. More precisely, the values of latitudes φ (in the range, 0–90°) and meridians ψ (in the range, 0–180°) of the most probable orientation of reticular

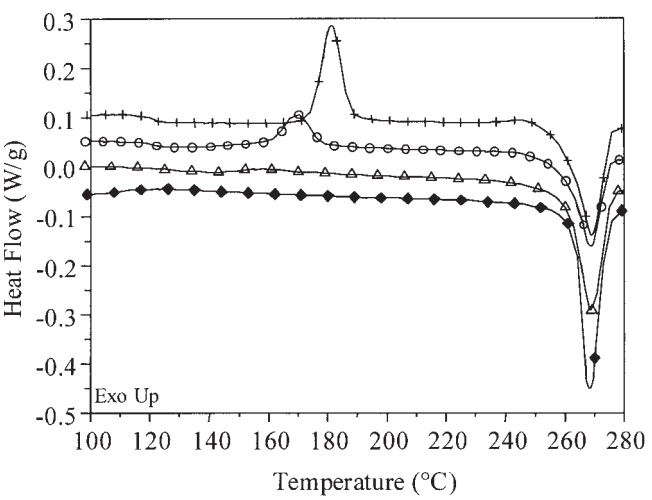

Figure 4 Selected curves from DSC data, respectively, of an unstretched amorphous (not shifted vertically) PEN (+), 1602 (●), 1603 (△), and 1004 (◆) samples (curves are shifted for clarity and symbols do not represent data points but are only a guide for the eye).

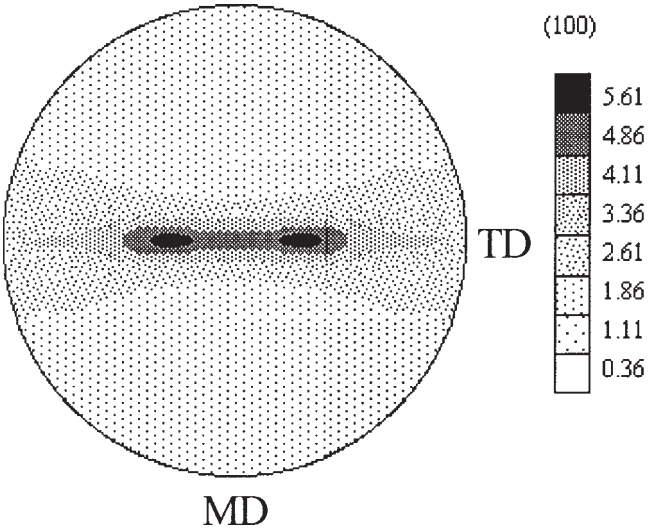

Figure 5 Scheme of (1 0 0) reticular plane pole figure for 1604 sample.

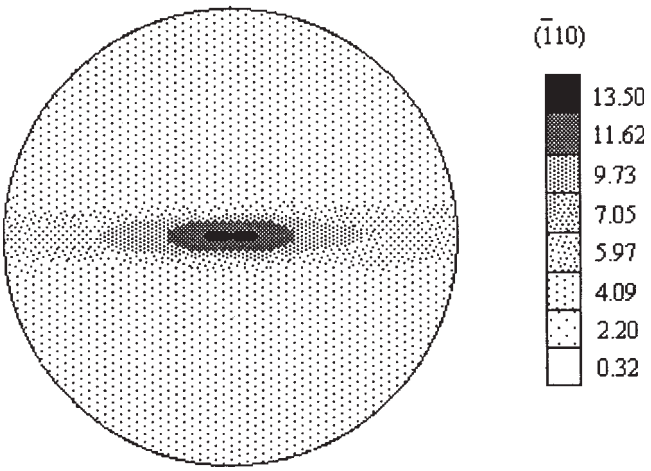

Figure 7 Scheme of (−1 1 0) reticular plane pole figure for 1604 sample.

planes (1 0 0), (0 1 0), (−1 1 0), (−3 0 6), and (−2 2 5) are summarized in Table V.

The pole figures of (0 1 0) show two different orientations of crystals in the film.

The main orientation displayed by Figure 3 corresponds to a plane of the chain (defined by the coplanar naphthalene ring) that is parallel to the film because the angle between the (−1 1 0) pole and the *OZ* direction = ND is close to 7.11° which is also the angle between (−1 1 0) and the chain plane (see Fig. 1).

The other population corresponds to a (0 1 0) orientation perpendicular to the main population of (0 1 0) planes, but still at $\psi = 90°$, thus with a naphthalene plane perpendicular to the plane of the film (Fig. 6). This trend was more pronounced for the films stretched at 100°C and for the highest drawing ratios, revealing a different crystallinity development scenario, possibly with a nucleation of ''daughter'' lamellae on the surface of primary crystals, the nucleation rate being higher at lower temperatures. Moreover, this difference in orientation comes with other morphological differences of the films. Indeed, the fibrillar morphology is better defined after stretching at 160°C than at 100°C (SAXS results display a two point diagram only after drawing at 160°C, not shown here), and the size and/or degree of perfection of the PEN crystals is clearly higher after high temperature drawing. At last, cavitation occurs after drawing below T_g at 100°C, and corresponds to a large increase of the apparent volume of the films (up to 40%). This cavitation is likely to change the stress/strain distribution in the films at the scale of the voids, and could play a role in the crystalline orientation that become close to uniaxial orientation with axis symmetry after stretching at 100°C.

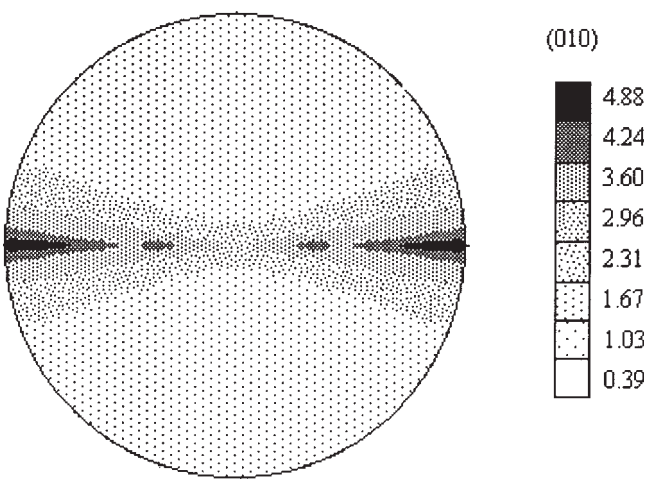

Figure 6 Scheme of (0 1 0) reticular plane pole figure for 1604 sample.

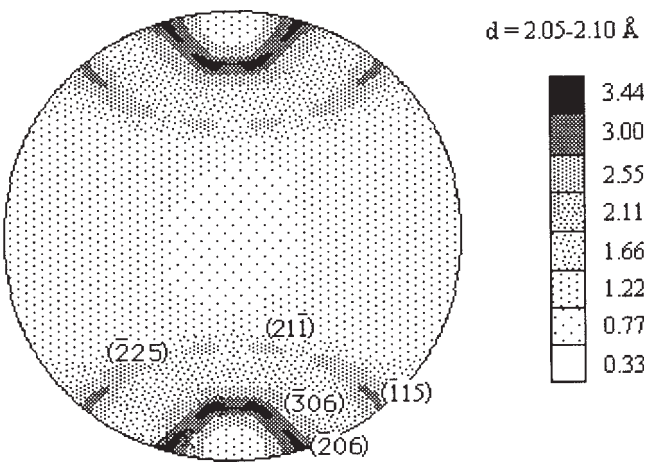

Figure 8 Scheme of multiple (−2 0 6) reticular plane pole figure for 1604 sample.

TABLE V
Latitude (φ) and Meridian (ψ) Coordinates of the Main Poles in Stretched PEN Samples

Sample	φ_{100}	ψ_{100}	φ_{010}	ψ_{010}	φ_{-110}	ψ_{-110}	φ_{-306}	ψ_{-306}	φ_{-225}	ψ_{-225}
100 1	69 and 111	90	16 and 164	90	76 and 104.5	90	24	5	16	35
100 2	69 and 111	90	16 and 164	90	76 and 104	90	24	5	16	35
100 3	68 and 112	90	17 and 163	90	77 and 103.5	90	23	5	17	35
100 4	67 and 113	90	18 and 162	90	78 and 102.5	90	23	5	18	35
100 4*	23 and 157	90	72 and 108	90						
160 1	–	–	–	–	–	–	–	–	–	–
160 2	69 and 111	90	16 and 164	90	76 and 104	90	24	5	16	36
160 3	68 and 112	90	17 and 163	90	77 and 103	90	23	5	17	35
160 4	67 and 113	90	18 and 162	90	78 and 102	90	21	5	18	35
160 4*	23 and 157	90	72 and 108	90		90				

Table V gives quantitatively the orientation cosines of the main population of PEN crystals. The secondary population is given for (1 0 0) and (0 1 0) reticular planes in the case of the samples at DR = 4 (labeled 1004* and 1604* in Table V), at right angle of the main set. Table VI gives the angles between some poles and also support this interpretation.

Contrarily to the conclusion in Ref. 5 that a crystalline texture with two orientation populations is due to a two-step transverse drawing in PEN bistretched films, a texture with two orientation groups also in the case of uniaxially stretched films is observed here.

Calculations of the orientation functions, according to eqs. (2) and (4), are listed in Table VI, and Figure 9 shows the orientation diagram of Wilchinski[9] associated with the chain axis orientation. It is clear that crystalline texture appears earlier, at DR = 1.5, for 100°C drawing, whereas 1601 sample is quite amorphous and weakly oriented. For the highest drawing rate, the orientation is more and more similar between 100 and 160°C up to DR = 4.

As a general trend, the orientation appears mainly with the *c* axis in the MD direction and the naphthalene ring in the plane of the film, i.e., its normal parallel to the *OZ* axis, a smaller population of naphthalene planes being perpendicular to the film. The orientation is thus uniplanar-axial as described by Murakami et al.[10] This result is qualitatively similar to previous observations of the orientation of the phenyl rings in PET,[11,12] although in this latter case orientation is obtained after rolling the films. The main population is in the orientation of the single crystal having naphthalene plane in the plane of the film. As all orientations still occur statistically in the film, a 2D-diffraction diagram can still be recorded (with an incident beam perpendicular to the film), as shown in Figure 10, but the intensity distribution is modified by the preferential uniplanar-axial orientation. As a result, as observed by Murakami et al.,[10] the variation of the equatorial diagram during the drawing process neither strictly behaves as a powder diagram, nor as true fiber diagram with axis of symmetry.

CONCLUSIONS

After studying the orientation of different uniaxially stretched PEN films, thus with different crystalline orientations by X-ray diffraction, the following conclusions can be drawn:

Pole figure measurements have shown mainly uniaxial orientation of the crystalline phase of PEN films after stretching.

In the range from DR = 2 to 4, the orientation is clearly uniplanar-axial. As a general trend, the orientation appears mainly with the *c* axis in the MD direction and the naphthalene ring in the plane of the film, i.e., its normal parallel to the ND axis, a smaller population of naphthalene planes being perpendicular to the film. Similar results have been found in PET.[13]

TABLE VI
Average Values of $\cos^2(\varphi_{h\ k\ l,\mathrm{MD}})$ for (1 0 0), (0 1 0), and (−1 1 0) Planes, as well as Averages Characterizing the Orientation of the *c* Axis, Namely $\cos^2(\vec{c}, OZ)$ with *OZ* = TD, ND, and MD, Respectively

Sample	$\langle\cos^2(\varphi_{100,\mathrm{MD}})\rangle$	$\langle\cos^2(\varphi_{010,\mathrm{MD}})\rangle$	$\langle\cos^2(\varphi_{-110,\mathrm{MD}})\rangle$	$\langle\cos^2(c,\mathrm{TD})\rangle$	$\langle\cos^2(c,\mathrm{ND})\rangle$	$\langle\cos^2(c,\mathrm{MD})\rangle$
100 1	0.221	0.268	0.205	0.217	0.270	0.513
100 2	0.203	0.247	0.184	0.197	0.247	0.556
100 3	0.136	0.211	0.125	0.131	0.211	0.658
100 4	0.124	0.184	0.104	0.114	0.184	0.702
160 1	0.297	0.253	0.300	0.300	0.253	0.447
160 2	0.175	0.253	0.112	0.194	0.253	0.552
160 3	0.150	0.201	0.125	0.144	0.201	0.650
160 4	0.168	0.184	0.106	0.156	0.184	0.660

For samples stretched below T_g, the crystallinity and orientation are higher than those of samples stretched above T_g.

Finally, in complement to a previous conclusion that a crystalline texture with two orientation populations is induced by to a two-step transverse drawing in PEN bistretched films,[5] a texture with two orientation groups is also observed here in the case of uniaxially stretched films: a main orientation which corresponds to a plane of the chain (defined by the coplanar naphthalene ring) that is parallel to the film. The other population corresponds to a (0 1 0) orientation perpendicular to the main population of (0 1 0) planes, but still at $\psi = 90^\circ$, thus with a naphthalene plane perpendicular to the plane of the film. This trend was more pronounced for the films stretched at 100°C and for the highest drawing ratios. Concerning the orientation of $\vec{c}$ axis, the chains are almost parallel to the MD direction after uniaxial stretching, whereas a more complex orientation distribution is obtained after transverse stretching. The chain axis orientation is described by a double population of crystals respectively, oriented in the plane of the film, mainly in the TD direction, and the second population stays oriented along the MD (i.e., between MD $+45^\circ$ and MD -45° in the film plane). As a result, the effect of transverse drawing is to strongly reorient the *c* axis of PEN crystals, while maintaining the naphthalene rings in the plane of the film.

The authors thank Du Pont de Nemours (R. Adam) for providing the amorphous PEN samples. This work has been also performed in the frame of bilateral PICS (International Scientific Co-operation Program between Poland and France) exchange program. The authors thank ESRF and French CRG at ESRF (Cyrille Rochas, D2AM beamline) for the 2D-WAXS characterization.

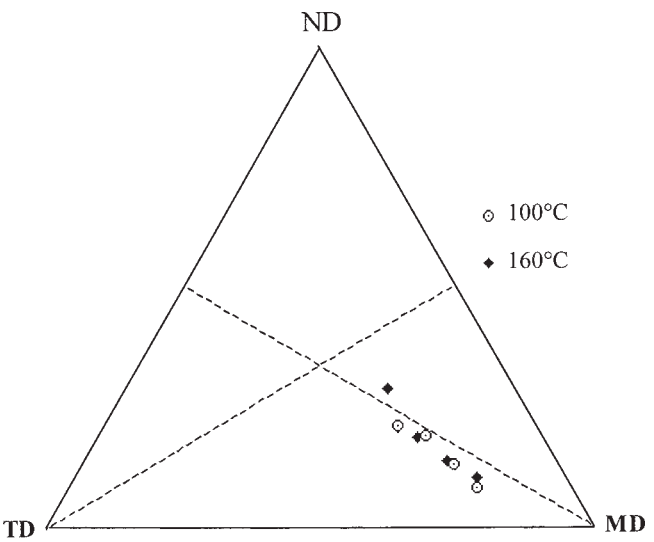

Figure 9 Orientation diagram of WILCHINSKI for the chain axis orientation in stretched PEN samples.

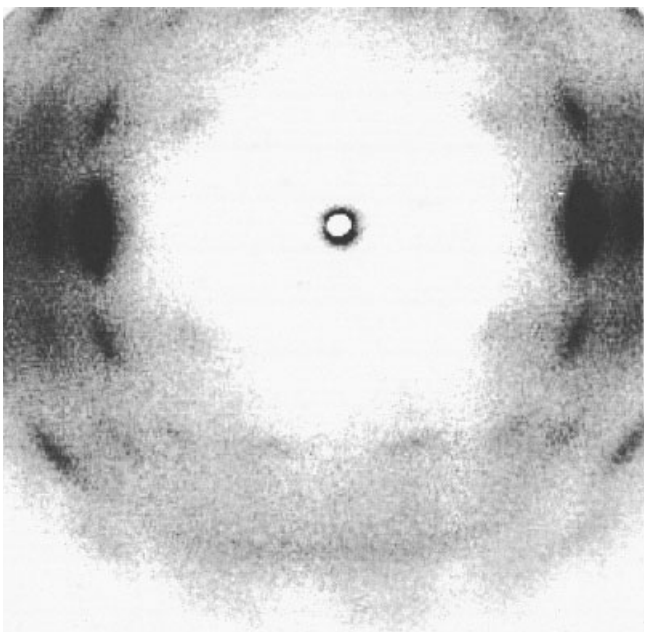

Figure 10 WAXS image of drawn PEN 1604 sample with film orientation perpendicular to incident beam, and drawing axis vertical (ESRF, BM2-D2AM beamline). The incident energy is 16 ke V. The main diffraction spot remains the (0 1 0) line that is close to Bragg orientation after stretching, whereas the powder of fiber diagram with axis symmetry would display the (1 0 0) as the more intense line. The low angle scattering (close to the beam stop) displays the two point scattering pattern characteristic of fibrillar morphology.

References

1. Krause, E. PhD Thesis (No. 2288), Université de Paul Sabatier, Toulouse, France, 1996.
2. Weick, B. L.; Bhushan, B. IEEE Trans Magn 1995, 31, 2937.
3. Weick, B. L.; Bhushan, B. Wear 1995, 190, 28.
4. Murakami, S.; Yamakawa, M.; Tsuji, M.; Kohjiya, S. Polymer 1996, 37, 3945.
5. Douillard, A.; Hardy, L.; Stevenson, I.; Boiteux, G.; Seytre, G.; Kazmmierczak, T.; Galeski, A. J Appl Polym Sci 2003, 89, 2224.
6. Hakme, C.; Stevenson, I.; David, L.; Boiteux, G.; Seytre, G.; Schönhals, A. J Non-Cryst Solids 2005, 351, 2742.
7. Mencik, Z. Chemicky Prümysil 1967, roc17(42), cfs2.
8. Alexander, L. E. X-ray Diffraction Methods in Polymer Science; Wiley-Interscience: New York, 1969; p 198.
9. Wilchinski, Z. W. Advances in X-ray Analysis; Plenum: New York: 1963; Vol. 6.
10. Murakami, S.; Nishikawa, Y.; Tsuji, M.; Kawaguchi, A.; Kohjiya, S.; Cakmak, M. Polymer 1995, 36, 291.
11. Lapersonne, P.; Tassin, J. F.; Monnerie, L. Polymer 1991, 18, 3321.
12. Lapersonne, P.; Bower, D. I.; Ward, M. I. Polymer 1992, 33, 1266.
13. Cakmak, M.; Lee, S. W. Polymer 1995, 36, 4039.
14. Hardy, L.; Stevenson, I.; Boiteux, G.; Seytre, G.; Schönhals, A. Polymer 2003, 44, 4311.
15. Hardy, L.; Fritz, A.; Stevenson, I.; Boiteux, G.; Seytre, G.; Schönhals, A. J Non-Cryst Solids 2002, 305, 174.
16. Hardy, L.; Stevenson, I.; Voice, A.; Ward, I. Polymer 2002, 43, 6013.